Search for UHE Photons with the Telescope Array Hybrid Detector

Katsuya Yamazaki[*] **for the Telescope Array collaboration**[†]

Earthquake Research Institute, The University of Tokyo, Tokyo, Japan
E-mail: kyamazaki@eri.u-tokyo.ac.jp

The origin of ultra-high energy cosmic rays are still unknown, and this is one of the biggest problem in the area of ultra-high energy cosmic ray research field. One of the reasons is magnetic deflection, because most of the cosmic rays are charged particles and the universe is filled with galactic and extragalactic magnetic fields. On the other hand, there is no magnetic deflection to the photons, so that their trajectories can be traced back to their origins. Therefore, we search for ultra-high energy photons with the Telescope Array experiment in order to understand origin of ultra-high energy cosmic rays. The Telescope Array is a hybrid detector consisting of an array of scintillation detectors, which measure the lateral profile of air showers, and fluorescence detectors, which measure the longitudinal profile of air showers. We use a parameter called X_{max}, which is the depth of maximal point of shower development, to search for photon-like events. We will report on the analysis method, and the result of a photon search using five years of TA data.

---

[*]Speaker.

[†]For full author list see http://www.telescopearray.org/images/papers/ICRC2015-authorlist.pdf

1. Introduction

The origin of ultra-high energy (UHE) cosmic rays has been sought for many years, and it is one of the most important topics in the UHE cosmic ray research field. Recently, the Telescope Array (TA) experiment has published a result consistent with the existence of anisotropy in the arrival directions of UHE cosmic rays However, sources of UHE cosmic rays are still unknown. One of the reasons is magnetic deflection in their trajectories. Since, the universe is filled with galactic and extragalactic magnetic fields, charged particles are deflected by these magnetic fields even though they are UHE cosmic rays. On the other hand, photons are not deflected by magnetic fields, and their trajectories can be traced back to their origins.

UHE photons have not been discovered yet, however, UHE photon emission is predicted by some UHE cosmic ray source models. There are basically two types of models. One is the non-acceleration model called "top-down" scenario. For instance, decay/annihilation of the relic Topological Defects (TD)[2] and Super Heavy Dark Matter (SHDM)[3], or resulting from resonant production of Z boson (Z-Burst, ZB)[4]. In contrast, the other type of model involves acceleration and is known as "bottom-up" scenario. In this scenario, UHE photons is produced by the GZK process from π^0 decays. These scenarios can be distinguished by the different flux of UHE photons. The UHE photon fluxes expected for the top-down models are significantly larger than that for bottom-up scenario. Also, within these scenarios we can examine the ratio of UHE photons to other UHE cosmic rays.

In this work, we search for UHE photons using the air shower profile observed by Fluorescence Detectors (FDs) in the Telescope Array (TA) experiment.

2. Telescope Array Experiment

The Telescope Array (TA) experiment is the largest observatory for UHE cosmic rays in the northern hemisphere, and it is located at 39.3° N, 112.9° W, and about 1400 m above sea level, Utah, USA. The experiment is operated by the international collaboration of Japan, USA, Korea, Russia, and Belgium, since 2008. TA consists of three fluorescence detector (FD) stations[5] and an array of 507 surface detectors (SDs)[6]. The area covered by the SD array is about 700 km^2, and the FDs are located at around the SD array viewing over the SD array. The FDs and SDs observe cosmic ray air showers, and each sampled data are used complementary to reconstruct the air showers with hybrid analysis method.

3. Monte Carlo Simulation for Hybrid Event

There are three steps for the hybrid event simulation in this work: simulation of extensive air showers (EASs), calculation of detector responses for SDs, and detector response simulation for FDs.

EASs are simulated with CORSIKA package[7]. For primary cosmic rays of energies above 10^{18} eV, the number of secondary particles becomes too large to trace all of the particles. Therefore, we use the *thinning* option to reduce the number of secondary particles to trace. The thinning factor of 10^{-6} is used for CORSIKA simulation in this work. The hadronic interaction model used in this work is *QGSJETII-03*[8].

The thinning causes non-trivial fluctuation to the lateral distribution of secondly particles. In order to correct this situation, a method has been developed by the TA collaboration to recover the information lost by thinning and to successfully use thinned showers for practical simulations, and this process is called *dethinning*[9]. Dethinned CORSIKA simulations are used for the SD response simulations using GEANT4. Each CORSIKA shower is used repeatedly with random different core positions to reduce the calculation time. For SD simulations with proton primaries, each proton shower is also used repeatedly with random different azimuthal angle. On the other hand, for photon primaries, the CORSIKA showers are not used repeatedly with azimuthal angle, because shower development depends on their azimuthal angles because of preshower effect[10], which causes electron-positron pair production by interacting with geomagnetic field at above the atmosphere.

The longitudinal development of EASs simulated with CORSIKA is used in the FD simulations using a software developed by the TA collaboration. Energy depositions are converted to fluorescence photons taking into account the wavelength spectrum, and parameterized atmospheric conditions. These photons are traced to the PMTs on FDs and simulated signals are produced.

4. Hybrid Event Reconstruction

The hybrid event reconstruction consists of four steps[11]: PMT selection, shower geometry reconstruction, longitudinal shower profile reconstruction, and quality cuts. The timing information of one triggered SD and time profile obtained by FDs are used to reconstruct the shower geometry. It allows significant improvement in the accuracy of the determination of shower geometries compared with the FD monocular analysis.

After the geometrical reconstruction, the longitudinal profile of the EAS is reconstructed using the FD data. In order to reconstruct longitudinal profile, reconstructed geometry and FD PMT signal profile are used in the Inverse MC (IMC) technique[12]. This IMC technique iteratively searches for the optimum parameters of longitudinal profile, which best matches the observed shower image.

There are inaccurately reconstructed events even though reconstruction process is successfully finished. For example, for an event of which true X_{max} is outside of the field of view (FOV) of FDs, it is difficult to estimate X_{max} with accuracy. Therefore, we discard these inaccurately reconstructed events from data set in order to avoid using these inaccurate events for further analyses. Additional quality cuts for the event selection are as follows:

- The number of selected PMTs > 20
- The estimated X_{max} is inside of the FOV of the FD
- The estimated incident zenith angle < 55 degrees
- The estimated core position is inside of the SD array
- The minimum viewing angle (see text) > 20 degrees

The minimum viewing angle is the minimum angle between the shower axis and the viewing angle from the FD to the each point of shower axis within the inside of the FOV. This cut reduces events which have photon component dominated by the Cherenkov photons, because for such events, because it is difficult to reconstruct the longitudinal profile of fluorescence photons with accuracy for such events.
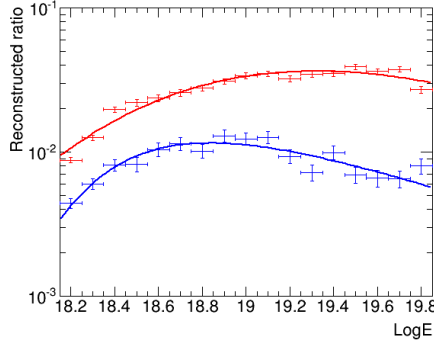
Figure 1: The survival fraction R. Red and blue points indicate R for protons and that for photons, respectively. The lines show the fit results with an empirical equation.

5. Photon-like Event Selection

Our quality cut requires the reconstructed X_{max} to be inside the FOV of FDs, thus deeply-penetrating EASs are discarded by this criterion because the shower maximum position may be lower than the FOV. Since most of EASs of primary photons have significantly deeper X_{max} than that of primary protons at energies greater than 1 EeV, photon primary EASs are more likely to be discarded with this criterion. Therefore, we applied an additional cut criterion discarding the events which have smaller reconstructed zenith angle than $20°$ (*photon enhancement cut*), to suppress acceptance bias between protons and photons. The acceptance bias is calculated comparing the survival fraction, R, for photon primaries to that for proton primaries. The fraction R is defined as the ratio of the number of remaining events after the reconstructions and quality cuts to the number of thrown MC events, *i.e.*, $R = N_{reconstructed}/N_{thrown}$. Figure 1 shows R for proton and photon primaries. As a result, we get the acceptance bias as the ratio of R for photons to that for protons (QGSJETII-03) as 0.312, 0.302, 0.280, and 0.248 at energies grater than 2, 3, 5, and 10 EeV, respectively.

After the photon enhancement cut, a photon-like event selection criterion is determined by MC simulation for photon primaries. We calculated the averages of reconstructed X_{max} for photon MC, and adopted it to the photon selection criterion. Figure 2 (left) shows the averaged X_{max} of the photon primary EASs. The fitting result of the averaged X_{max} of each energy bin for the photon primaries is the photon selection criterion in this work. When the reconstructed X_{max} of an EAS is larger than the selection criterion at the energy range of the event, the event is tagged as photon-like event. Selection efficiencies for primary photons are 0.476, 0.477, 0.500, and 0.479 at energies greater than 2, 3, 5, and 10 EeV, respectively. In Figure 2 (right), the selection criterion and reconstructed X_{max} of proton primary EASs are plotted. In order to estimate the proton contamination with this photon selection criterion, the photon selection is applied to the proton MC (QGSJETII-03) data set. Then, 3.1%, 1.1%, 0.9%, and 0.9% protons are tagged as photon-like events at energies greater than 2, 3, 5, and 10 EeV, respectively.

The period of the observed data set is from May 2008 to July 2013. In this work, I used the data obtained by two FD stations, BR and LR, and the SD array. Figure 3 shows X_{max} of observed events together with the line denoting the photon-like event selection criterion. The events of which X_{max}
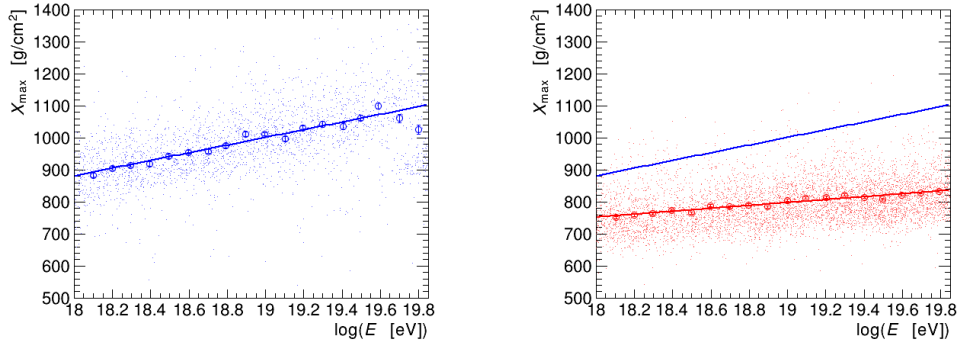
Figure 2: (Left) The blue dots are X_{max} values of photon-induced EASs. The blue open circles show the averaged X_{max} at each energy bin, the size of each bin is 0.1 in logarithm of energy. The blue line shows the fitting results of photon averaged X_{max}. (Right) The red dots are reconstructed X_{max} for MC simulated events of primary protons, and blue line is the selection criterion determined by left figure. Open circles show the averaged X_{max} of protons at each energy bin, the size of each bin is 0.1 in logarithm of energy.
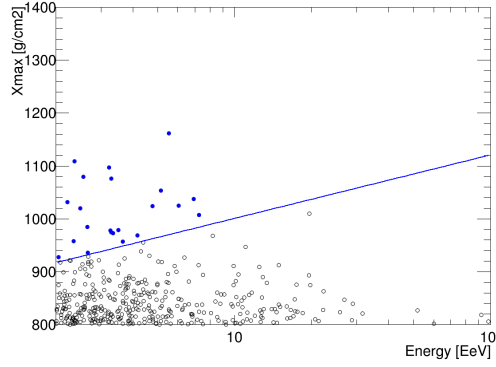
Figure 3: Reconstructed X_{max} of observed events and the selection criterion. The circles show data points and the line is the selection criterion described in this section. The observed data passed the quality cuts and the photon enhance cut.

values exceed the criterion line are selected as photon-like events. The numbers of the photon-like events are 22, 14, 5, and 0 in the energy ranges with energies greater than 2, 3, 5, and 10 EeV, respectively. The numbers of all events which passed quality cuts are 1525, 830, 371, and 123 in the same corresponding energy ranges, respectively.

An individual photon-like event selected according to the criteria above can not be definitively identified as a photon. It is expected that some protons have deeper X_{max} than the selection criterion due to fluctuation of a longitudinal development. Thus, we compared the number of photon-like events with the expected number of photon-like event from deeply penetrating proton EASs. In order to estimate the proton contamination, the same selection is applied to the proton MC made with QGSJETII-03. As a result, the expected numbers of photon-like events with proton MC are 47.1, 8.7, 3.3, and 1.1 with energy ranges grater than 2, 3, 5, and 10 EeV, respectively.

6. Photon Fraction Upper Limit

The upper limit of the photon fraction, which is the fraction of photon flux to all particle flux, is calculated with selection results in this section. In order to obtain a conservative upper limit, the photon-like events are assumed to be caused by primary photons. This is because the $X_{\max}$ distribution of protons highly depends on which high energy hadronic interaction model is used, thus we can not estimate realistic contamination from protons without systematic uncertainty.

The upper limit of the number of photon-like events using the Poisson distribution is calculated assuming no background, *i.e.*, all the photon-like events are assumed to be photons. Poisson upper limits of the number of photon-like events with 95% confidence level are obtained as 31.4, 21.9, 10.5, and 3.0 in the range with energies above 2, 3, 5, and 10 EeV, respectively. As discussed above the photon selection of this analysis discards not only nuclei but also photons, thus the selection efficiency should be taken into account for calculating the upper limit. As a results we obtained 95% confidence level upper limits of the numbers of photon-like events, $n_\gamma|_{95\%}$, as 66.0, 45.9, 21.0, and 6.3 in the range with energies above 2, 3, 5, and 10 EeV, respectively.

Finally, we obtained the upper limit of photon fraction with 95% confidence level, $F_\gamma|_{95\%}$, from the following relation,

$$F_\gamma|_{95\%} = \frac{I_\gamma|_{95\%}}{I_\gamma|_{95\%} + I_p} = \frac{n_\gamma|_{95\%}}{n_\gamma|_{95\%} + (n_{\mathrm{obs}} - n_\gamma|_{95\%})A_\gamma/A_p}, \qquad (6.1)$$

where I_γ and I_p are the fluxes of photons and protons, respectively, n_{obs} indicates the number of observed events, n_γ is the number of the photon-like events, A_γ and A_p are the apertures of the experiment for primary photons and protons, respectively, and the notation of "95%" means 95% confidence level upper limit. The ratio of the apertures, A_γ/A_p, is substituted from the acceptance ratio derived in Section 5. Then, the upper limits of the photon fractiona with 95% confidence level are obtained as 12.7%, 16.3%, 17.7%, and 17.8% in energies above 2, 3, 5, and 10 EeV, respectively. The results of the calculations are summarized on Table 1. Figure 4 is the photon fraction upper limit comparing to other experimental results and predictions from several models. In this figure, the result from the same processes of analysis as this work with monocular data set, which are reconstructed with the monocular method, is also shown.

There are systematic uncertainties on energy determination with the hybrid analysis. It consists of uncertainties of the detector calibration, the atmospheric attenuation, the fluorescence yield, and the reconstruction error. The total systematic uncertainty on energy determination is calculated with the quadratic sum of these uncertainties, and that is 21%. In order to estimate the systematic uncertainty on the photon fraction upper limits, the upper limits are recalculated with shifting the energy scales by -42%, -21%, $+21\%$, and $+42\%$. Then, we can find that systematic shift on upper limits in each energy range is +2.5%, +0.0%, +1.8%, and +29.5% in energies above 2, 3, 5, and 10 EeV.

7. Conclusion and Future Work

The studies for EASs of primary photons and searching for UHE photons using $X_{\max}$ with hybrid reconstruction technique are presented in this work. This is the first result which measured by the hybrid detection technique in the northern hemisphere.

Table 1: The results of the photon fraction upper limits with 95% confidence level. See text for details.

	> 2 EeV	> 3 EeV	> 5 EeV	> 10 EeV
The number of photon-like events, n_γ	22	14	5	0
Poisson fluctuation with 95% c.l.	31.4	21.9	10.5	3.0
Photon selection efficiency	0.476	0.477	0.500	0.479
Upper limit of the number of photon-like events with 95% c.l. $n_\gamma\vert_{95\%}$	66.0	45.9	21.0	6.3
Acceptance ratio, A_γ/A_p	0.312	0.302	0.280	0.248
The number of all data, n_{obs}	1525	830	371	123
The upper limit of the photon fraction with 95% c.l., $F_\gamma\vert_{95\%}$ (%)	12.7	16.3	17.7	17.8
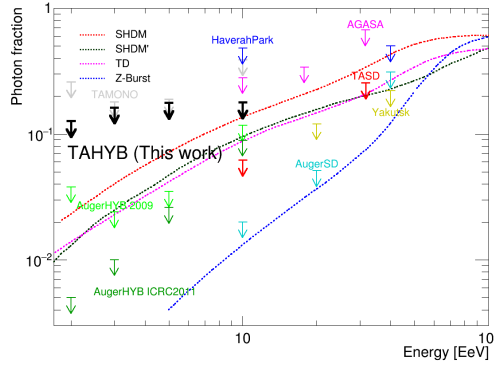
Figure 4: Photon fraction upper limits. Black arrows show the results of this work. The other arrows show other experimental results: gray is the TA monocular analysis result, red is the TA SD analysis result[13], light green is the Auger hybrid result presented in 2009[14], green is the Auger hybrid result presented in 2011[15], light blue is the Auger SD result[16], blue is the Haverah Park[17, 18], yellow is the Yakutsk[19, 20], and pink is the AGASA result[21, 22]. The lines show the predictions from top-down models [23, 24, 25].

As a result of this work, the predicted photon fractions with top-down scenarios are not constrained. However, in consideration of combination with the TA SD result, which search for photon candidates by using waveform feature collected by SDs, SHDM models and TD model of the UHECR generation are constrained with 95% confidence level, and Z-burst model are survived with these upper limits in the northern hemisphere. It is important that independent search of UHE photons in the northern and the southern hemisphere, because UHE photons are expected to be anisotropically observed since sources or generation points of UHE photons are limited to near to the Earth due to their mean free path, and also they are not deflected by the magnetic fields in the universe.

In future analysis, we will include information of secondary particles at the ground, such as lateral distribution and shape of waveform derived as SD observable, and then it is expected that the discrimination power of photons from nuclei is improved, and a photon likeness of each event

can be estimated.

Acknowledgements

References

[1] R. Abbasi *et al.*, *The Astrophysical Journal Letters*, **790**, L21, 2014.

[2] M. B. Hindmarsh and T. W. B. Kibble, *Reports on Progress in Physics*, **58**, p. 477, 1984.

[3] M. Birkel and S. Sarkar, *Astroparticle Physics*, **9**, pp. 297–309, 1998.

[4] T. J. Weiler, *Astroparticle Physics*, **11**, pp. 303–316, 1999.

[5] T. Abu-Zayyad *et al.*, *Nuclear Instruments and Methods in Physics Research A*, **676**, pp. 54–65, 2012.

[6] T. Abu-Zayyad *et al.*, *Nuclear Instruments and Methods in Physics Research A*, **689**, pp. 87–97, 2012.

[7] D. Heck *et al.*, *CORSIKA: A Monte Carlo Code to Simulate Extensive Air Showers*, Forschungszentrum Karlsruhe Report FZKA 6019, 1998.

[8] S. Ostapchenko, *Nuclear Physics B Proceedings Supplements*, **151**, pp. 143–146, 2006.

[9] B. T. Stokes *et al.*, *Astroparticle Physics*, **35**, pp. 759–766, 2012.

[10] T. Erber, *Review of Modern Physics*, **38**, pp. 626–659, 1966.

[11] T. Abu-Zayyad *et al.*, *Astroparticle Physics*, **61**, pp. 93–101, 2015.

[12] T. Fujii *et al.*, *AIP Conference Proceedings*, **1367**, pp. 149–152, 2011.

[13] T. Abu-Zayyad *et al.*, *Physical Review D*, **88**, 112005, 2013.

[14] The Pierre Auger Collaboration, *Astroparticle Physics*, **31**, pp. 399–406, 2008.

[15] K. Kampert *et al.*, "Highlights from the Pierre Auger Observatory", *Proceedings of 32st International Cosmic Ray Conference*, 2011.

[16] J. Abraham *et al.*, *Astroparticle Physics*, **29**, pp. 243–256, 2008.

[17] M. Ave *et al.*, *Physical Review Letters*, **88**, pp. 2244–2247, 2000.

[18] M. Ave *et al.*, *Physical Review D*, **65**, 063007, 2002.

[19] A. V. Glushkov *et al.*, *JETP Letters*, **85**, pp. 131–135, 2007.

[20] A. V. Glushkov *et al.*, *Physical Review D*, **82**, 041101, 2010.

[21] K. Shinozaki *et al.*, *The Astrophysical Journal*, **571**, L117, 2002.

[22] M. Risse *et al.*, *Physical Review Letters*, **95**, 171102, 2005.

[23] G. Gelmini *et al.*, *Journal of Experimental and Theoretical Physics*, **106**, 11, 2008.

[24] J. Ellis *et al.*, *Physical Review D*, **74**, 115003, 2006.

[25] M. Risse *et al.*, *Physics Letters A*, **22**, 749, 2007.